Aqueous micellar solution to control non-solvent–solvent exchange during phase inversion process of polysulfone membrane preparation resulting in membranes of different pore structures

Puyam S. Singh* and Kripal Singh

CSIR Central Salt and Marine Chemicals Research Institute, RO Membrane Division, G.B. Marg, Bhavnagar 364 002, India

The study reports the preparation of polysulfone membranes of very precise and uniform pores and pore size distribution. The concentration of *N,N*-dimethylformamide (DMF) and sodium dodecyl sulphate (SDS) surfactant in the coagulation bath played a vital role in pore formation during phase inversion process. Polysulfone membranes of narrow pore size distribution with median pores at about 0.04–0.06 μm were obtained.

Keywords: Casting process, polysulfone membrane, micellar solution bath, narrow pore size distribution.

MEMBRANES are commonly porous polymeric materials used because of its low-cost, effectiveness and reliability in many industrial separation processes[1–5]. The characterization of membranes for fundamental properties such as pore size and pore size distribution is therefore extremely important for tailoring membrane for specific separations. Polysulfone membranes are widely used in membrane separation processes because of their high mechanical strength, good thermal stability, and resistance to acid/alkali solutions. To make a polysulfone membrane with precise pore size and narrow pore size distribution to achieve an effective sieving with an acceptable fluid flow is a challenging task. Generally polysulfone membranes are prepared by solution casting phase inversion technique. Studies on the preparation of polysulfone and sulfonated polysulfone membranes by phase inversion processes have been reported earlier[6,7]. The phase inversion process involves precipitation of homogeneous polymer solution or a stable colloidal dispersion (casting solution) in a coagulation bath. The casting (liquid) solution is obtained by dissolving the polymer in a good solvent while the colloidal casting solution is the liquid solution with an appropriate amount of a non-solvent. The membrane is casted by spreading the casting liquid as a thin layer on a suitable support followed by application of a coagulating liquid onto the casting surface. Two types of phase inversions occur during the process[8]: (a) absorption of non-solvent water from air moisture while casted as a thin layer and (b) immersion of the polymer solution into a coagulation (non-solvent) bath. The effects of coagulation conditions[9], thermodynamic conditions[10] during formation of polysulfone membranes as well as phase separation[11] and phase diagrams[12] of polysulfone/solvent/water have been discussed earlier.

Asymmetric polysulfone membranes having numerous 0.005–3 μm surface pores and symmetric microporous polysulfone membranes having 0.1–0.2 μm pores have been prepared by selective combination of casting and coagulating solution conditions[13,14]. Another report reveals that polysulfone membranes of pore sizes ranging from 0.002 to 10 μm can be generated from a polysulfone solution (15 wt%) in *N*,*N*-dimethylformamide (DMF), by fast or slow demixing in water or water vapour[15]. Separate studies[16,17] have shown that polysulfone membranes formed by coagulating a polysulfone solution (15 wt%) in *N*-methyl-2-pyrrolidone (NMP) with water vapour possess pore sizes from 5 to 12 μm (ref. 16) whereas the membrane formed by coagulating a polysulfone solution (14 wt%) in NMP with pure water possesses pore size of about 0.1–0.2 μm (ref. 17). Commercially available polysulfone membranes have non-uniform pore structures and its pore sizes are typically larger than 0.2 μm (ref. 18).

Kinetics of phase separation for 15–25 wt% of polysulfone solutions in *N*-methyl-2-pyrrolidone with water vapour was studied using time-resolved small angle light scattering and phase contrast optical microscope and it suggests a bicontinuous network structure having pore sizes of few microns[19]. Using atomic force microscopy, it has been shown[20] that polysulfone membrane formed by coagulating a polysulfone solution (20 wt%) in *N*-methyl-2-pyrrolidone (NMP) with water or a mixed water/NMP as coagulants has different pore structures. The membrane prepared from pure water coagulant has nodular

*For correspondence. (e-mail: puyam@csmcri.org)

structures of about 0.025 μm nodule size and the pores formed at the interstitial regions between the nodules are about 0.01–0.02 μm in diameter. The membrane prepared from the coagulant comprising mixed water–NMP solution has a large pore structure of about 0.2 μm in diameter.

Recently, effects of aqueous coagulation bath containing ethanol or glacial acetic acid on properties of modified polysulfone membrane casted from polysulfone–dimethylacetamide solution were reported[21]. The results indicated that adjusting coagulation bath composition is an effective approach to tailor the membrane properties.

In the present study, the effect of aqueous coagulation bath containing DMF and sodium dodecyl sulfate (SDS) micelles on the pore characteristics of polysulfone membrane casted from polysulfone–DMF solution, is reported. Coagulation baths of different water–DMF–SDS compositions were taken for the study. The capillary porometry method was used to mainly characterize membrane pore characteristics and the results are presented.

Theory

Preparation of polysulfone membrane from polymer solution by phase inversion process using a coagulation bath of aqueous micellar solution is studied. Different compositions of micellar solution from water, DMF and SDS were used to observe the influence of coagulating solution properties on the final membrane properties. The changes in solution properties in terms of surface tension and Gordon parameters for the water–DMF mixtures used as the bulk phase in the micellar solutions were studied (Figure 1).

The Gordon parameter values used to characterize self-association of conventional amphiphiles were calculated from the solvent surface tension and molar volume data. The calculated values were larger than the value of $1.2\ J\ m^{-3}$ required for micellization indicating that, SDS micelles in the solution could occur[22]. Figure 2 shows correlation plots of critical micelle concentration (CMC) of the SDS micelles as a function of DMF content in the different water–DMF micellar solutions using the experimental data[23–25]. Increase in the concentration of micelles but decrease in the size of aggregates with increase in the amount of polar organic solvent is generally observed[22–25]. Thus, it can be concluded that water–DMF mixtures can contain different concentrations of micelles and sizes of micellar aggregates.

Thus, there are changes in the solution properties for the aqueous micellar solution mixture used as a coagulating medium for the phase inversion process of membrane preparation. The activity of water is reduced in the aqueous solution with increase in DMF content which changes the diffusional exchange rate between water (non-solvent) of coagulation bath and solvent (DMF) of the polymer solution during the phase inversion process. Based on differences in the diffusional exchange rate, different types of membrane structures can be formed. As shown in Figure 3, high shrinkage of the membrane can occur with abrupt loss of solvent by fast exchange with non-solvent while membrane of low shrinkage can be obtained with slow and gradual release of solvent. In turn, it can generate low or high compressive force which can directly influence the packing density of the polymer nodular structures of the membranes formed. Additionally, micelles from aqueous solution can also diffuse into the polymer film during the process. Thus, the micelles can be trapped in the ternary phase of water–DMF–polymer as shown in Figure 4 that can subsequently affect the pore structure of the final membrane.

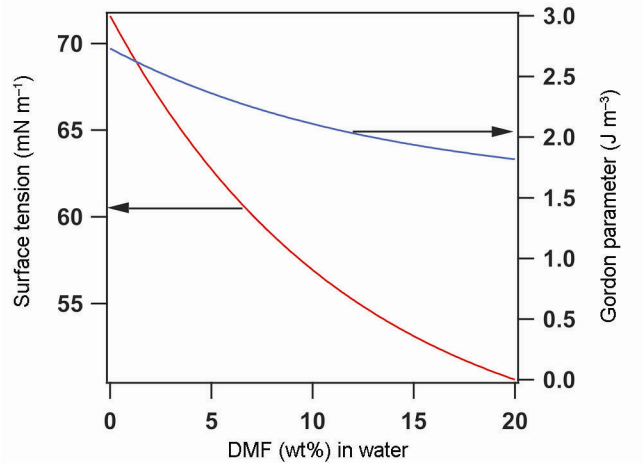

Figure 1. Changes in the solution properties in terms of surface tension and Gordon Parameter as a function of DMF content in water.

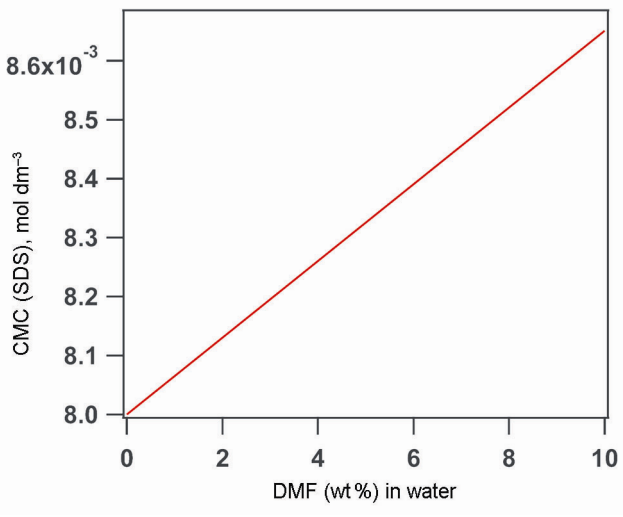

Figure 2. A correlation plot of critical micelle concentrations (CMC's) of the SDS micelles as a function of DMF content of the water–DMF micellar solution (plot is constructed based on the experimental results of refs 23–25).

Experimental

Casting of polysulfone membranes

Polysulfone solution was prepared by dissolving 15 wt% Udel P-3500 polysulfone (Union Carbide, USA) in A.R. grade DMF. The resultant polymer solution was cast on a non-woven fabric Nordyls T-100 from a water bath consisting of a fixed amount of DMF and SDS surfactant using phase inversion process. Casting was done in a continuous mode using a casting unit developed here as described elsewhere[26,27].

The enclosed casting chamber of the casting unit was maintained at a temperature of about 36°C and relative humidity of about 22%. Polysulfone membrane samples of different pore characteristics were prepared from different conditions as given in Table 1.

The fabric was rolled from a supply roller in the casting base where the thin film of casting liquid was formed on the fabric. The cast liquid film on the fabric was then passed through a guide roller where the thickness of the film was controlled. After the casting chamber, the cast film was then immediately passed into the coagulation bath where liquid film was precipitated into solid membrane. The resulting polysulfone membrane was washed thoroughly with distilled water.

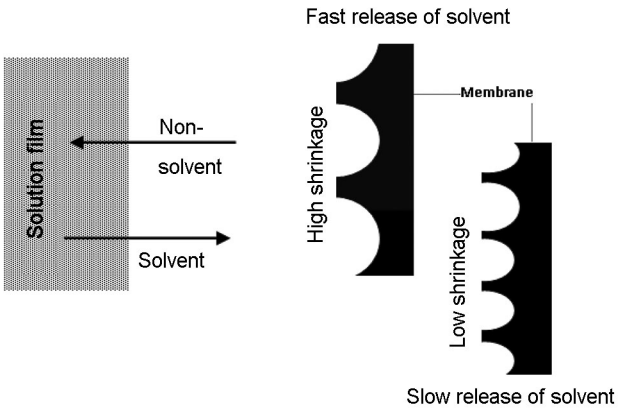

Figure 3. Schematic representation of low and high shrinkage of the membrane.

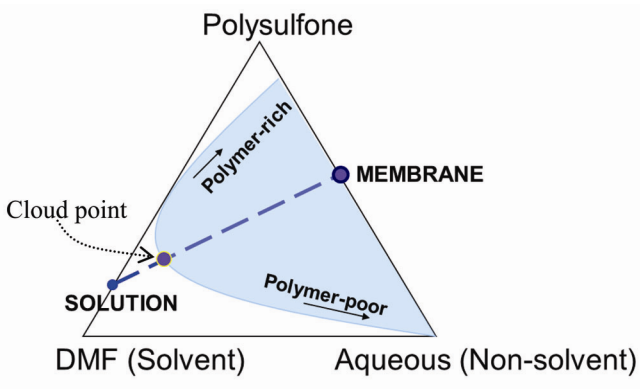

Figure 4. A typical ternary phase diagram of water–DMF–polymer of membrane formation.

Characterization of membrane pore structure

Mean flow pore size, bubble point, cumulative flow and pore size distribution of the samples were performed using a PMI (Porous Materials, Inc. USA) capillary flow porometer. Circular samples from the membrane were cut and soaked in 'Porewick', a pore wetting liquid supplied by PMI. The samples were soaked overnight to ensure that all pores in the samples were filled with fluid. The sample was then placed at the bottom of the sample chamber completely covering the bottom O-ring. The sample fits between the two O-rings. Any gas flowing through the sample will be constrained by these two O-rings to flow-up and out of the top of the sample chamber. Gas flowing out the sides of the sample will be trapped by the large, side O-ring grinding the 'spacing insert' and will not escape to the atmosphere causing pressure loss and a falsely high flow rate. The 'spacing insert' then presses the sample down. Finally, the cap is screwed onto the chamber and tightened to the point where the O-ring on top of the 'spacing insert' is compressed against the chamber cap. The gas inlet pressure was then adjusted and measurement started with CAPWIN software system supplied by PMI.

The capillary flow porometry method is quick and simple for characterization of porous materials, and frequently used for pore size analysis of commercial membranes[28,29]. This method has been approved as an ASTM procedure for characterization of porous materials including membrane filters[30]. The theory of this method is briefly described here. The less wetting fluid under an applied pressure can displace the more wetting fluid held in the pores of membrane according to Laplace equation

$$\Delta p = 2\gamma H, \tag{1}$$

where γ is the interfacial tension of the fluid–fluid system, and H the mean curvature of the meniscus.

Table 1. Coagulation bath conditions of the polysulfone membrane samples

Sample	Solvent composition (%, w/w)		cmc (SDS; 25°C)
	DMF	Water	mol dm^{-3}
PS1	2.0	98.0	0.00813
PS2	3.7	96.3	0.00824
PS3	6.0	94.0	0.00839
PS4	7.5	92.5	0.00849
PS5	9.1	90.9	0.00859

In the case of a spherical meniscus in a cylindrical pore, the Laplace equation resulted in Washburn equation, is also known as Cantor's equation

$$\Delta p = \frac{4\gamma \cos\theta}{d}, \tag{2}$$

where d is the pore diameter and θ the contact angle between the membrane surface and liquid. The pores of membranes are typically modelled as cylindrical capillaries and in such a case $J(d)$, the volume flow rate for pores of diameter d, can be expressed by the Hagen–Poiseuille equation[31]

$$J(d) = \frac{\phi}{32}\frac{d^2\Delta p}{\psi\eta l}, \tag{3}$$

where ψ is the constriction–tortuosity factor, η the fluid viscosity, l the membrane thickness and ϕ, the porosity is given by the equation

$$\phi = \frac{\pi}{4}\sum_{j=1}^{n} N(j)d^2(j), \tag{4}$$

where $N(j)$ is the density of pores of diameter d.

Using eqs (3) and (4), the total number of pores in the sample can be determined; however, an assumption has to be made about the geometry of the membrane pores for extraction of membrane tortuosity factor. If the membrane sample pores are excessively constricted, the pore counts may be statistically low whereas, if the pores are asymmetrical then the pore number density may be overcalculated. Therefore, in our analysis of capillary porometer data, the pore number densities of the samples are not determined. Instead, the relative pore size distributions of samples are determined using a normalization procedure from the flow-pressure curve and this procedure does not need the assumption of pore geometry. The normalization procedure is detailed as follows. The cumulative filter flow, ΣQ is given by the ratio of wet flow rate and dry flow rate. The filter flow, ΔQ between pores of diameter d_2 at pressure p_2 and pores of diameter d_1 at pressure p_1 is the difference between cumulative filter flows at pressure p_2 and p_1. A plot of $\Delta Q/\Delta d$ against the pore diameter, d gives pore size distribution curve.

SEM pictures of the samples were taken using LEO 1430VP scanning electron microscope with 5 kV accelerating voltage. Atomic force microscopy (AFM) images of the samples were acquired using NT-MDT AFM instrument. The polysulfone membranes were evaluated for pure water flux on a batch type water permeability test kit comprising of four cells in series. The circular membrane samples with a diameter of 4.8 cm were placed on a porous stainless steel sintered support disc in the test cell, with a rubber O-ring around it to ensure leak-free operation.

Results

Capillary flow porometer data

The wet flow porometer flow as a function of pressure for five polysulfone membrane samples are shown in Figure 5. Up to a pressure difference of about 45 psi, the wetting liquid acts as a barrier and no flow is seen. The appearance of first bubbles is known as 'bubble point pressure'. After this, there is a progressive increase in flow rates with pressure, and at a higher pressure, the wet flow rates increase sharply and meet the dry flow rates. The curves display the theoretical 'S shape' of the 'flow–pressure curve'. The bubbles first appear from the liquid saturated membrane when the test gas pushes the liquid out of the largest sized pores at higher pressures of 62–64 psi for samples PS1 and PS2, than 46–50 psi for other samples (sample PS3, PS4 and PS5). Thus, according to eq. (2), the largest pore size (also known as bubble point pores) present in samples PS1 and PS2 is about 0.1 μm, whereas it is about 0.14 μm for the other samples (Table 2). The 'S-shaped' wet flow-pressure curves are observed for the samples, where the liquid from the smallest sized pores 0.040 μm is emptied at about 160 psi for sample PS1 and from relatively larger 0.057 μm pores is emptied at 116 psi for sample PS5. The smallest sized pores present in the samples PS2, PS3 and PS4 are respectively 0.046, 0.050 and 0.055 μm, which are midway between the sizes of PS1 and PS5.

The pressure ranges from the 'bubble point pressure' to the first inflection point and before the upward swing of the curve are 62–160 psi for sample PS1, 48–138 psi for sample PS2 and 46–107 psi for samples PS3, PS4 and PS5. The steep portions between the first and second inflection point of the curves have different slopes. The results are indicative of samples having different pore sizes and pore size distributions as given in Table 2.

The progressive summing of the wet filter flow is the cumulative filter flow. The correlations of cumulative filter flow against the pore size for the samples are examined. Smooth curves through the points with only one point of major inflection are obtained in the plots. This may represent smooth pore size distribution of the main pores (MP). The MP size range determined from the analysis was 0.04 to 0.07 μm. The pore size distributions for the samples can be clearly seen from the plots of $\Delta Q/\Delta d$ (differential filter flow/differential diameter) against the pore diameter (Figure 6). For each sample, a sharp peak in the range of 0.04 to 0.07 μm of the MP was clearly distinctive from the broad distribution of low intensity peaks of other bigger pores of sizes $0.07 <$ 0.12 μm in diameter. About 57% of the total pores for the

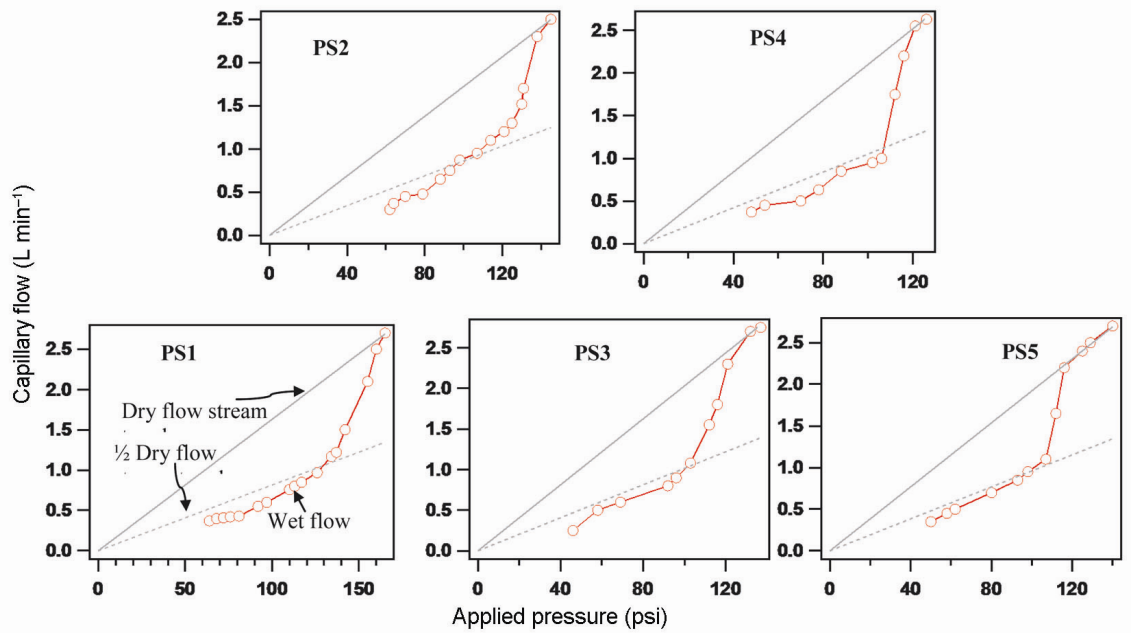

Figure 5. The wet flow porometer flow as a function of pressure for five polysulfone membrane samples.

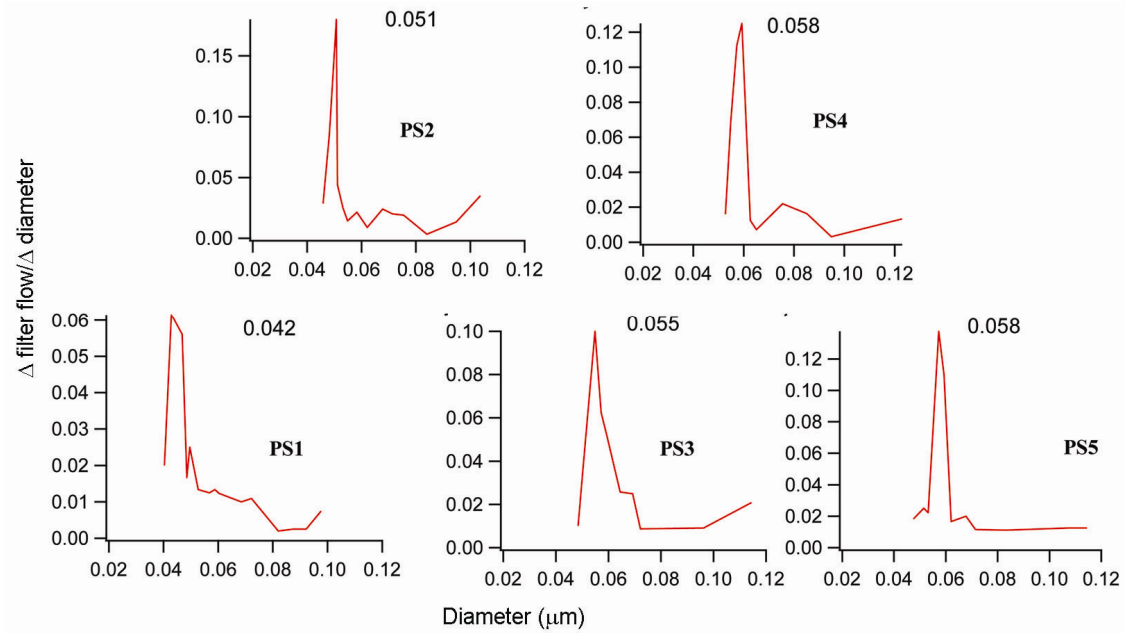

Figure 6. The pore size distributions for the five membrane samples.

Table 2. Porosity analysis of the membranes

Membrane	PS1	PS2	PS3	PS4	PS5
Smallest pore diameter (μm)	0.040	0.046	0.050	0.055	0.057
Mean flow pore diameter (μm)	0.051	0.060	0.063	0.069	0.070
Bubble point diameter (μm)	0.104	0.107	0.144	0.138	0.132
% Distribution of majority of pores	56.69	63.99	89.18	66.67	61.57
Diameter range of majority of pores (μm)	0.040–0.048	0.045–0.055	0.050–0.072	0.055–0.065	0.057–0.062
Cumulative wet flow (l/min)	17.85	16.44	12.48	11.25	8.75

sample PS1 are in MP range of 0.040–0.048 μm with median pore at 0.042 μm while the larger pores of 0.11 > 0.048 μm make up the remaining percentage of the total pores. In case of the sample PS2, the main pores that constitute about 64% of the total pores are slightly bigger 0.045–0.055 μm with median pore size 0.051 μm than that of the sample PS1. A larger majority of 87% of total pores as the MP with median pore at 0.055 μm are observed for the sample PS3, although the distribution of these MP is relatively wider in the range of 0.050–0.072 μm in comparison with the samples PS4 and PS5. Relatively, narrow pore size distribution but bigger sizes 0.055–0.065 μm of the main pores with median pore at 0.058 μm constituting about 62–67% of the total pores are observed for samples PS4 and PS5 containing more DMF and SDS micelles. These observations indicate a wide distribution of pores in PS1 and PS2 membranes and a comparatively narrow distribution in PS3, PS4 and PS5 membranes. This implied that the membrane prepared by precipitating in coagulating solution having least concentration of DMF and SDS micelles contained wide distribution of pores in comparison to those precipitated in coagulating solution having higher concentrations of DMF and SDS micelles. Thus, the formation of pores in the membrane is influenced by the concentration of DMF and SDS in coagulating solution.

Other measurements

Pure water permeability (PWP) data for the samples are evaluated. Wide variations (the standard deviation near to the average value of 12 test coupons measurements of each sample type) in the PWP data among the test coupons for samples PS1 and PS2 are observed. The pure water flux of the membranes measured at an operating pressure of 50 psi is shown in Figure 7. This may be an indication of pore size non-uniformity of the separating membrane layer in samples PS1 and PS2. In comparison, variations of the water flux data in the test coupons were fewer in samples PS3, PS4 and PS5, which may indicate the existence of better pore size uniformity in these samples. The ratio of the fluxes for samples PS3, PS4 and PS5 is 1.0 : 1.1 : 1.0. This shows similar porosity of these samples based on the relationship between the porosity and permeability according to eqs (3) and (4).

The porous structures of the samples are also examined by SEM micrographs. While a clear distinction of nanoscale surface features among samples is beyond the resolution limit of our SEM instrument used here, the surface morphology for PS3, PS4 and PS5 samples was found to be more homogeneous than those of PS1 and PS2 samples. The membrane has a denser top layer with a porous sub-layer. The top layer comprises nodular structures and the pores are formed between the interstitial regions of the nodules, similar to other previous results[20]. Uniform distribution of pores was not seen in samples PS1 and PS2 whereas uniformly distributed pore network structures were observed in samples PS3, PS4 and PS5. A representative SEM micrograph of the membrane surface is shown in Figure 8. However, clear differences among the samples in terms of surface pore sizes and numbers were difficult to be characterized by our SEM instrument used here.

In order to further characterize the surface morphology of the samples, AFM surface images of the samples were measured. Figure 9 shows the AFM images of the samples of scan size 10 μm × 10 μm. The statistical characteristics for the surfaces were estimated by roughness analysis of the AFM surface images (Table 3).

The surface roughness parameters of the samples are in the range of 4–6 nm and therefore, the sample surfaces can be considered as quite smooth. A slight increase in the peak-to-peak distance of the surface roughness parameter was observed for samples in the order of PS5 > PS4 > PS3 > PS2 ~ PS1. Surface–depth profiles of the samples from section analysis of the AFM surface

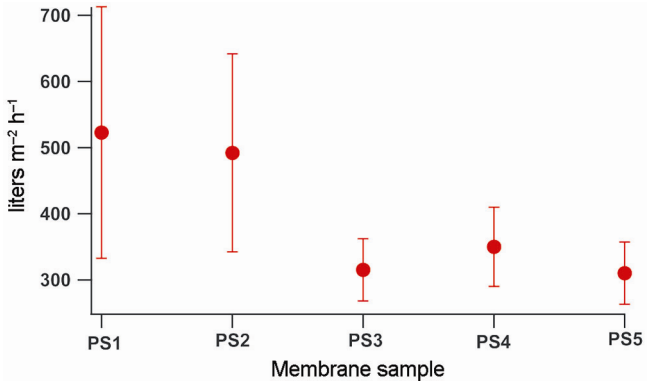

Figure 7. Pure water flux of the membranes at 50 psi.

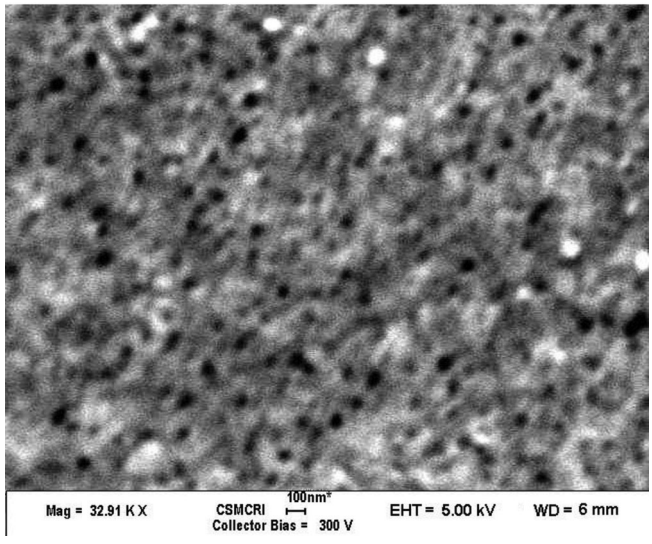

Figure 8. A representative SEM micrograph of the polysulfone membrane surface.

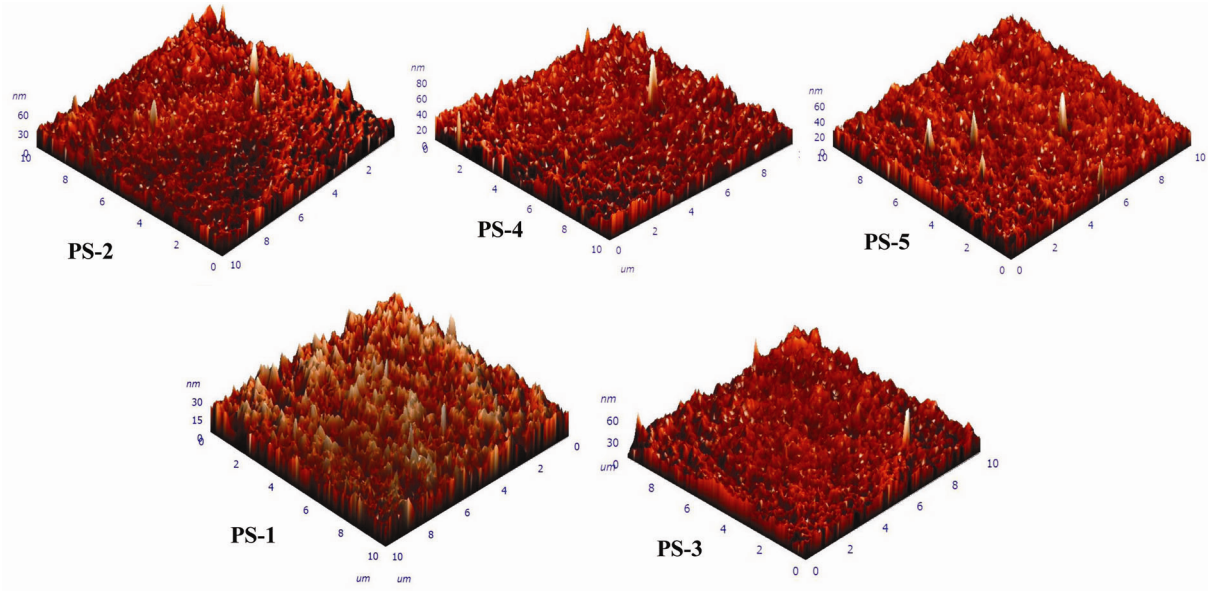

Figure 9. AFM surface images of the membrane samples.

Table 3. Surface roughness properties of the membranes

Properties	PS1	PS2	PS3	PS4	PS5
Peak to peak maximum distance (Sy), nm	78	78	88	92	98
Mean value of peak to peak distance (μ), nm	20	20	22	26	33
Average arithmetic roughness (Sa), nm	5.0	4.0	4.0	5.3	4.2
Root mean square roughness (Sq), nm	6.3	5.3	5.4	6.8	5.6

images are shown in Figure 10. The pore asymmetry nature of the samples can be examined from the surface–depth profiles where the larger surface pores and the smaller active pores are marked by dotted lines and solid lines respectively. From an analysis of the profiles, the pore asymmetry of the samples can be compared. It revealed that the pore asymmetry for sample PS1 was the highest. The pores of samples PS3, PS4 and PS5 were found to be more symmetric.

Discussion

For the aqueous coagulation bath containing low DMF content (<4 wt%), the polysulfone membrane (PS1) formed exhibited a wider range of pores while the polysulfone membrane of uniform porosity was formed from the coagulation bath containing an appropriate DMF (10 >4 wt%). We further observed (not presented here) that the polysulfone membrane formed from the coagulation bath containing higher DMF content (>10 wt%) had lesser amount of active pores for permeation.

As mentioned above, the DMF content in the 'aqueous coagulation bath' is important in controlling pore size uniformity and porosity of the polysulfone membranes formed by the phase inversion process. The formation of membrane pore structure is mainly dependent on concentration-dependent Flory–Huggins interaction parameters for the aqueous/DMF, DMF/polysulfone and aqueous/polysulfone systems[10]. For an uncontrolled preparation, membrane pores may be formed in interstitial regions between the aggregated nodules or constricted pores, and in some cases, the presence of non-connected pore networks (macrovoids) in the membranes may exist.

The solidification rate of the liquid film immersed into the micellar aqueous bath after casting can be different because of the difference in the diffusional exchange rate between water and DMF. According to the Wilke–Chang equation, the calculated diffusivity of water to DMF was 1.58×10^5 cm^2/s while the diffusivity of DMF to water was 0.91×10^5 cm^2/s (refs 15, 32). Therefore, as the DMF content increased in the aqueous coagulation bath, the diffusivity of the aqueous solution is decreased, delaying the demixing of the phase inversion process of membrane formation. Secondly, the CMC of the SDS micelle in the aqueous coagulation bath increased with increased DMF content resulting in greater association of water in micellar aggregates thereby further delaying the demixing process. This type of phase separation by delayed demixing can generate closed pores which do not work as active pores for permeation while fast demixing can generate more number of flow-through pores responsible for permeation[15]. This is exactly what has been observed in the case

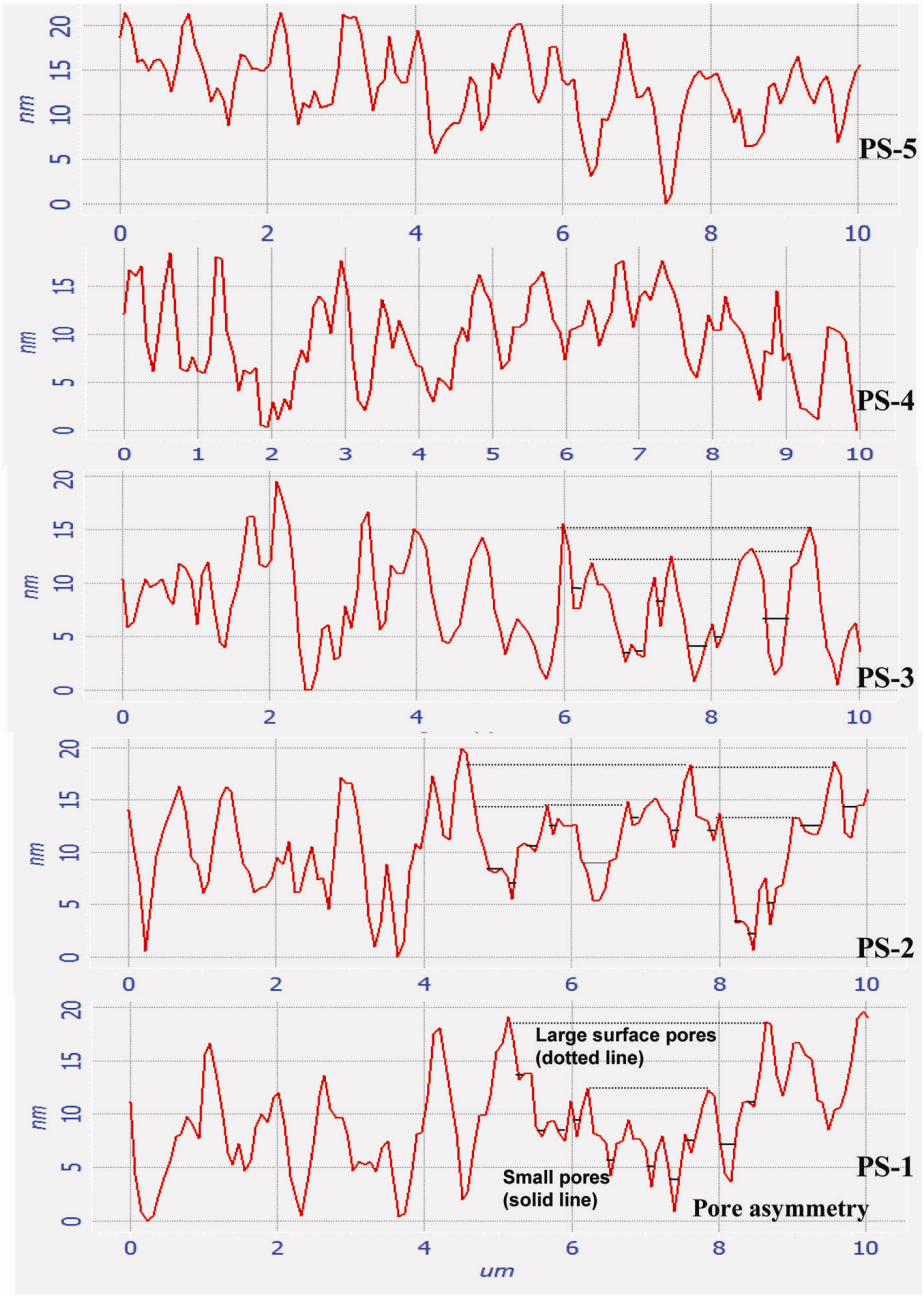

Figure 10. Surface-depth profiles of the samples from section analysis of the AFM surface image.

of membrane PS1 prepared with the coagulating bath containing the lowest DMF where it had the highest overall capillary wet-flow. The capillary wet-flow decreased for membrane samples in the order of PS1 > PS2 > PS3 > PS4 > PS5 in line with increased DMF content in the coagulating bath. Effect of adding N-methyl pyrrolidone (NMP) solvent in aqueous coagulation bath to the reduction of polysulfone membrane pore voids by direct microscopic observation was reported recently[33].

Secondly, the PS1 membrane exhibited majority of the smallest pores and a wider pore range. This can be explained as follows. Abrupt loss of solvent by fast exchange with non-solvent can generate high compressive force which can increase amplitude of the solid surface resulting in a range of pores. On the other hand, an increase in the amount of SDS micelles incorporated during solidification of the process may increase the structural ordering of the polymer nodules assembled on the regular structure of the micelles. Thus, the PS5 membrane obtained using the coagulating bath containing the highest amount of SDS micelles exhibited the narrowest pore size distribution of MP. The results agree with other studies[34] on a different casting system that showed macrovoid formation in polysulfone membrane can be

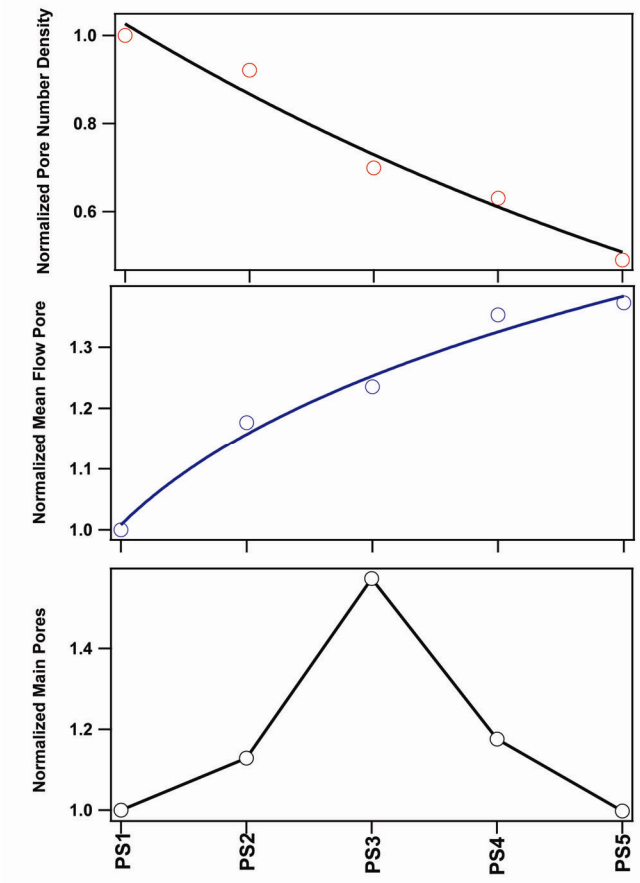

Figure 11. Comparison plots for the membranes in terms of main-pores, mean–flow–pore and pore–number–density by normalizing with the corresponding values of the PS1 membrane.

suppressed by addition of surfactant (Span-80) in the casting solution as a result of change in interfacial properties between the coagulant and the polymer solution.

The effect of DMF-micelle content on the porous properties of the membranes in terms of MP, mean–flow–pore and pore–number–density is compared by normalizing with the corresponding values of PS1 membrane. The comparison plots are shown in Figure 11. The MP of sizes 0.04 to 0.07 μm in diameter almost increased by 50% for the PS3 membrane obtained by using coagulation bath containing 6 wt% DMF and CMC (SDS) of 8.39×10^{-3} mol dm^{-3} as compared to that of PS1 membrane obtained from coagulation bath containing 2 wt% DMF and CMC (SDS) of 8.13×10^{-3} mol dm^{-3}. On the other hand, the change in total porosity of the membranes is relatively less affected because of increase or decrease in mean–flow–pore or pore–number–density respectively.

Conclusions

It is observed that polysulfone membrane of uniform pore structure can be obtained using an appropriate composition of aqueous micellar solution of water–DMF–SDS as coagulating medium for the phase inversion process of membrane preparation. An uncontrolled preparation may produce polysulfone membrane with an ineffective sieving and an unacceptable fluid flow. The composition of coagulation solution indicated noticeable effect on the pore formation in the membrane during precipitation. Low concentration of DMF in coagulation solution resulted in a wide range of pores and higher concentration of DMF resulted in narrow pore distribution. Uniformly distributed pore network structures are observed in samples PS3, PS4 and PS5 compared to PS1 and PS2 membranes obtained by phase inversion process from the initial polysulfone solution (15%, w/w) in DMF. Further improvement in pore size uniformity of the membrane was achieved by SDS surfactant incorporation in the membrane. This may be because of 'delayed demixing' between solvent and non-solvent since both DMF and surfactant of the aqueous coagulating solution contributed to decrease in activity of water. At the same time, the 'delayed demixing' can generate closed pores which do not work as active pores for permeation while the fast demixing can generate more number of 'flow-through' active pores. Therefore, optimum concentration of DMF along with surfactant is essential to prepare a membrane of desired pore structure. Among the membranes studied, the PS3 membrane prepared using coagulation bath of 6 wt% DMF is the best in terms of pore size uniformity, which exhibited 87% of the total active pores as MP in 0.050–0.072 μm range with median pore at 0.055 μm.

1. Ho, W. S. W. and Sirkar, K. K., *Membrane Handbook*, Van Nostrand Reinhold, New York, 1992.
2. Kestlng, R. E., *Synthetic Polymer Membranes*, McGraw Hill, New York, 1972.
3. Lonsdale, J. K., The growth of membrane technology. *J. Membr. Sci.*, 1982, **10**, 81.
4. Humphrey, J. L. and Keller, G. E., *Separation Process Technology*, McGraw-Hill Publishers, NY, 1997.
5. Muralidhara, H. S. and Satyavolu, J., Reducing food processing costs in the 21st century: need for innovative separation technologies. *Ind. Eng. Chem. Res.*, 1999, **38**, 3710.
6. Cross, R. A., Dialysis membrane and its use, US Patent No. 3,691,068, 1972.
7. Marze, X., Polymeric compositions for membranes, US Patent No. 4,207,182, 1980.
8. Wilmans, J. G., Baaij, J. P. B. and Smolders, C. A., The mechanism of formation of microporous or skinned membranes produced by immersion precipitation. *J. Membr. Sci.*, 1983, **14**, 263.
9. Yamasaki, A., Tyagi, R. K., Fouda, A. E., Matsuura, T. and Jonasson, K., Effect of gelation conditions on gas separation performance for asymmetric polysulfone membranes. *J. Membr. Sci.*, 1997, **123**, 89.
10. Barth, C., Goncalves, M. C., Pires, A. T. N., Roeder, J. and Wolf, B. A., Asymmetric polysulfone and polyethersulfone membranes: effects of thermodynamic conditions during formation on their performance. *J. Membr. Sci.*, 2000, **169**, 287.
11. Lau, W. W. Y., Phase separation in polysulfone/solvent/water and polyethersulfone/solvent/water systems. *J. Membr. Sci.*, 1991, **59**, 219.

12. Barth, C. and Wolf, B. A., Quick and reliable routes to phase diagrams for polyethersulfone and polysulfone membrane formation. *Macromol. Chem. Phys*., 2000, **201**, 365.
13. Wrasidlo, W. J., Dispersing casting of integral skinned highly asymmetric polymer membranes, US Patent No. 4,774,039, 1988.
14. Ly, A. L., Chu, C. and Nguyen, T. D., Isotropic microporous polysulfone membrane. US Patent No. 4,970,034, 1990.
15. Han, M. J. and Bhattacharyya, D., Changes in morphology and transport characteristics of polysulfone membranes prepared by different demixing conditions. *J. Membr. Sci*., 1995, **98**, 191.
16. Park, H. C., Kim, Y. P., Kim, H. Y. and Kang, Y. S., Membrane formation by water vapor induced phase inversion. *J. Membr. Sci*., 1999, **156**, 169.
17. Wang, I. F., Ditter, J. F. and Morris, R. A., Highly asymmetric ultrafiltration membranes. US Patent No. 5958989, 1999.
18. Moaddeb, M. and Koros, W. J., Occlusion of pores of polymeric membranes with colloidal silica. *J. Membr. Sci*., 1997, **136**, 273.
19. Lee, H. J., Jung, B., Kang, Y. S. and Lee, H., Phase separation of polymer casting solution by nonsolvent vapor. *J. Membr. Sci*., 2004, **245**, 103.
20. Kim, J. Y., Lee, H. K. and Kim, S. C., Surface structure and phase separation mechanism of polysulfone membranes by atomic force microscopy. *J. Membr. Sci.*, 1999, **163**, 159.
21. Xu, J., Tang, Y., Wang, Y., Shan, B., Yu, L. and Gao, C., Effect of coagulation bath conditions on the morphology and performance of PSf membrane blended with a capsaicin-mimic copolymer, *J. Membr. Sci.*, 2014, **455**, 121.
22. Graciani, M. M., Munoz, M., Rodrıguez, A. and Moya, M. L., Water-*N*,*N*-dimethylformamide alkyltrimethylammonium bromide micellar solutions: thermodynamic, structural, and kinetic studies. *Langmuir*, 2005, **21**, 3303.
23. Benrraou, M., Bales, B. L. and Zana, R., Effect of the nature of the counterion on the properties of anionic surfactants. 1. CMC, ionization degree at the CMC and aggregation number of micelles of sodium, cesium, tetramethylammonium, tetraethylammonium, tetrapropylammonium, and tetrabutylammonium dodecyl sulfates. *J. Phys. Chem. B*, 2003, **107**, 14432.
24. Rodriguez, A., Graciani, M. M. and Moya, M. L., Effects of addition of polar organic solvents on micellization. *Langmuir*, 2008, **24**, 12785.
25. Almgren, M., Swarup, S., Lofroth, J. E., Effect of formamide and other organic polar solvents on the micelle formation of sodlum dodecyl sulfate. *J. Phys. Chem.*, 1985, **89**, 4621.
26. Singh, P. S., Joshi, S. V., Trivedi, J. J., Devmurari, C. V., Rao, A. P. and Ghosh, P. K., Probing the structural variations of thin film composite RO membranes obtained by coating polyamide over polysulfone membranes of different pore dimensions. *J. Membr. Sci*., 2006, **278**, 19.
27. Veerababu, P., Vyas, B. B., Singh, P. S. and Ray, P., Limiting thickness of polyamide-polysulfone thin-film-composite nanofiltration membrane. *Desalination*, 2014, **346**, 19–29.
28. Schneider, K., Holz, W., Wollbeck R. and Ripperger, S., Membranes and modules for transmembrane distillation. *J. Membr. Sci*., 1988, **39**, 25.
29. Reichelt, G., Bubble point measurements on large areas of microporous membranes. *J. Membr. Sci*., 1991, **60**, 253.
30. ASTM F316: Standard test method for pore size characteristics of membrane filters by bubble point and mean flow pore test; ASTM E1294: Standard test methods for pore size characteristics of membrane filters using automated liquid porosimeter.
31. Mulder, M., *Basic Principles of Membrane Technology*, Kluwer, Dordrecht, The Netherlands, 1991.
32. Wilke, C. R. and Chang, P., Correlation of diffusion coefficients in dilute solutions. *AIChE J*., 1955, **1**, 264.
33. Guillen, G. R., Ramon, G. Z., Kavehpour, H. P., Kaner, R. B. and Hoek, E. M. V., Direct microscopic observation of membrane formation by nonsolvent induced phase separation. *J. Membr. Sci*., 2013, **431**, 212.
34. Tsai, H. A., Li, L. D., Lee, K. R., Wang, Y. C., Li, C. L., Huang, J. and Lai, J. Y., Effect of surfactant addition on the morphology and pervaporation performance of asymmetric polysulfone membranes. *J. Membr. Sci*., 2000, **176**, 97.

ACKNOWLEDGEMENTS. Financial support from CSMCRI as research grants (9/1/CS/CSMCRI(1)/2012-13-PPD). The instrumentation facility provided by the ‘Analytical Discipline and Centralized Instrument Facility’ of CSMCRI is also gratefully acknowledged.

Received 2 September 2015; revised accepted 27 November 2015

doi: 10.18520/cs/v110/i8/1485-1494